Rheol Acta 37:61–67 (1998)
© Steinkopff Verlag 1998

ORIGINAL CONTRIBUTION

Marios M. Fyrillas
Georgios C. Georgiou

Linear stability diagrams for the shear flow of an Oldroyd-B fluid with slip along the fixed wall

Received: 19 June 1997
Accepted: 22 September 1997

M.M. Fyrillas · G.C. Georgiou (✉)
Department of Mathematics and Statistics
University of Cyprus
P.O. Box 537
1678 Nicosia, Cyprus

Abstract We consider the time-dependent shear flow of an Oldroyd-B fluid with slip along the fixed wall. Slip is allowed by means of a generic slip equation predicting that the shear stress is a non-monotonic function of the velocity at the wall. The complete one-dimensional stability analysis to one-dimensional disturbances is carried out and the corresponding neutral stability diagrams are constructed. Asymptotic results for large values of the elasticity number and finite element calculations are also presented. The instability regimes are within or coincide with the negative-slope regime of the slip equation. The numerical calculations agree with the linear stability results when the size of the initial perturbation is small. Large perturbations may destabilize a linearly stable steady state, leading to a periodic solution. The period and the amplitude of the periodic solutions increase with elasticity.

Key words Shear flow – Oldroyd-B model – slip – linear stability analysis – asymptotic analysis

Introduction

In a recent paper, Georgiou (1996) numerically solved the time-dependent shear flow of an Oldroyd-B fluid with non-linear slip along the fixed wall, demonstrating that the combination of non-linear slip and viscoelasticity results in periodic solutions. This mechanism of instability may be used to explain some of the instabilities observed during the extrusion of polymer melts. Other mechanisms of instability have been proposed in the literature, in the past few years (Larson, 1992). Among them, the combination of slip and compressibility (Pearson, 1985; Hatzikiriakos and Dealy, 1992a, b; Georgiou and Crochet, 1994a, b) and constitutive instabilities (Malkus et al., 1991; Larson, 1992) are the most popular. The latter mechanism is restricted to constitutive models that predict a non-monotonic shear stress-shear rate relationship in steady shear flow.

The Oldroyd-B model exhibits a monotonic steady-shear response in the absence of slip and, therefore, the mechanism proposed in Georgiou (1996) is different from the constitutive instability mechanism that is based on the multi-valuedness of the stress constitutive equation (Malkus et al., 1991 and references therein). The instabilities are caused by the multi-valuedness of the slip equation, instead, and elasticity just provides the means to sustain the oscillations by storing and releasing elastic energy.

In Georgiou (1996), the stability of the steady-state solutions of the problem under study was investigated by means of a simple one-dimensional linear stability analysis and by finite element calculations. Certain constraints on the material parameters were imposed so as to avoid the existence of multiple steady-state solutions. It was found that the instability regimes are always within or coincide with the negative-slope regime of the slip equation. Both the linear stability analysis and the numerical calculations showed that the Newtonian solutions are everywhere stable and that the interval of instability grows as one moves from the Newtonian to the

RA 863

© Steinkopff Verlag 1998

upper-convected Maxwell model. Perturbing an unstable steady-state solution leads to periodic solutions, the amplitude and the period of which increase with elasticity. However, the numerical instability regimes were much broader than those predicted by the simple linear stability analysis. This is explained by the fact that, in solving the resulting eigenvalue problem, it was assumed that the eigenvalues were real. In the present work, we relax this assumption and obtain improved linear stability diagrams. The finite element calculations agree with the predictions of the present analysis when the size of the initial perturbation is small.

The governing equations and the boundary conditions for the time-dependent shear flow of an Oldroyd-B fluid with slip along the fixed wall are presented in the second section. The steady-state solutions are also given there. In the third and fourth sections, the linear stability analysis to one-dimensional disturbances is carried out and neutral stability curves are constructed for various values of the material parameters. In the fifth section, the asymptotic results for large values of the elasticity number are obtained. The linear stability results are compared with numerical calculations in the final section.

Governing equations

We consider the time-dependent shear flow of an Oldroyd-B fluid. The geometry and the boundary conditions of the flow are illustrated in Fig. 1. The two plates are separated by a distance H. The flow is assumed to be one-dimensional and, hence, only the x-component v_x of the velocity vector $\boldsymbol{v}$ is not zero. The extra stress tensor $\boldsymbol{T}$ and the velocity component v_x are functions of the y coordinate and the time t: $\boldsymbol{T}=\boldsymbol{T}(y,t)$ and $v_x = v_x(y,t)$. The lower plate moves with a constant speed V_1. It is assumed that no slip occurs along this wall and thus

$$v_x(0,t) = V_1 . \tag{1}$$

Along the upper plate, which is fixed, it is assumed that slip occurs according to the following generic slip equation:

$$\sigma_w = -F(v_w) \quad \text{at} \quad y = H , \tag{2}$$

where σ_w is the shear stress and v_w is the slip velocity of the fluid at the upper wall.

In the case of the Oldroyd-B model, the extra stress tensor is decomposed as follows (Crochet et al., 1984):

$$\boldsymbol{T} = \boldsymbol{T}_1 + \eta_2 [(\nabla \boldsymbol{v}) + (\nabla \boldsymbol{v})^{\mathrm{T}}] , \tag{3}$$

where $\boldsymbol{T}_1$ is the viscoelastic part, the second term in the RHS of Eq. (3) is the purely viscous part of the extra stress tensor $\boldsymbol{T}$, η_2 is a material parameter and the superscript T denotes the transpose. The tensor $\boldsymbol{T}_1$ is defined by

$$\boldsymbol{T}_1 + \lambda \left[\frac{\partial \boldsymbol{T}_1}{\partial t} + \boldsymbol{v} \cdot \nabla \mathrm{T}_1 - (\nabla v)^{\mathrm{T}} \cdot \boldsymbol{T}_1 - \boldsymbol{T}_1 \cdot (\nabla \boldsymbol{v}) \right] = \eta_1 [(\nabla \boldsymbol{v}) + (\nabla \boldsymbol{v})^{\mathrm{T}}] , \tag{4}$$

where η_1 and λ are material parameters. The shear viscosity is given by $\eta_1+\eta_2$. The Newtonian and the upper-convected Maxwell models are recovered by setting η_2 equal to 1 and 0, respectively.

Scaling the lengths by H, the velocity by a characteristic velocity V, the stress components by $(\eta_1+\eta_2)V/H$, and the time by H/V, leads to two dimensionless numbers, the Reynolds number

$$\mathrm{Re} \equiv \frac{\rho V H}{\eta_1 + \eta_2} , \tag{5}$$

where ρ is the density, and the Weissenberg number

$$\mathrm{We} \equiv \frac{\lambda V}{H} . \tag{6}$$

For the one-dimensional flow problem studied here, the x-component of the momentum equation and the xy- and xx-components of the constitutive Eq. (4) are written as follows:

$$\mathrm{Re} \frac{\partial v_x}{\partial t} = \frac{\partial \mathrm{T}_1^{xy}}{\partial y} + \eta_2 \frac{\partial^2 v_x}{\partial y^2} , \tag{7}$$

$$\mathrm{T}_1^{xy} + \mathrm{We} \frac{\partial \mathrm{T}_1^{xy}}{\partial t} = \eta_1 \frac{\partial v_x}{\partial y} , \tag{8}$$

$$\mathrm{T}_1^{xx} + \mathrm{We} \left(\frac{\partial \mathrm{T}_1^{xx}}{\partial t} - 2 \frac{\partial v_x}{\partial y} \mathrm{T}_1^{xy} \right) = 0 . \tag{9}$$

As pointed out in Georgiou (1996), Eq. (9) for T_1^{xx} is not coupled with Eqs. (7) and (8) and the yy stress

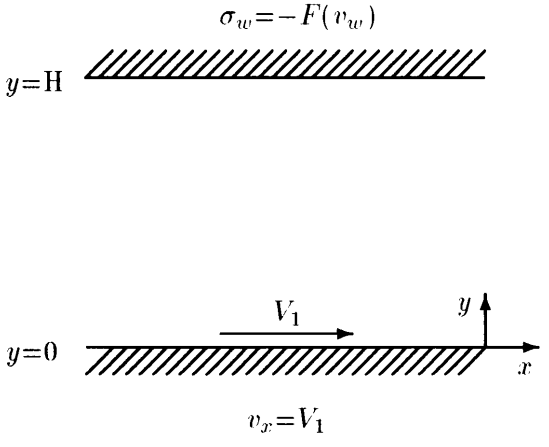

Fig. 1 Boundary conditions for the time-dependent shear flow with slip at the fixed wall

component T_1^{yy} is zero and remains so at all times provided the problem remains one dimensional. All the variables in the above three equations are dimensionless, including η_1 and η_2 which are scaled by the shear viscosity (the dimensionless shear viscosity $\eta_1 + \eta_2$ is equal to unity).

The steady-state solution is easily obtained. The velocity v_x varies linearly with y and the shear stress is constant:

$$v_x = V_1 + (v_w - V_1)\, y\,, \tag{10}$$

and

$$T^{xy} = v_w - V_1\,, \tag{11}$$

where the slip velocity v_w satisfies the condition:

$$v_w - V_1 = -F(v_w)\,. \tag{12}$$

Demanding that the velocity $V_1 = v_w + F(v_w)$ is a monotonic function of v_w or, equivalently, that the steady-state solution for a given value of V_1 is unique, leads to the following constraint for the slip function F:

$$F'(v_w) \equiv \frac{dF(v_w)}{dv_w} > -1\,. \tag{13}$$

Linear stability analysis

In this section, the stability of the steady-state solutions to one-dimensional infinitestimal disturbances is studied by means of a linear stability analysis. Let $(\bar{v}_x, \bar{T}_1^{xy})$ be a steady-state solution given by Eqs. (10) and (11), and $(\hat{v}_x(y)\, e^{\kappa t}, \hat{T}_1^{xy}\, e^{\kappa t})$ be a small one-dimensional perturbation. The sign of the real part of κ determines whether the perturbation will grow or decay over a finite period of time. From the time-dependent governing Eqs. (7) and (8), one obtains:

$$\mathrm{Re}\,\kappa \hat{v}_x = \frac{d\hat{T}_1^{xy}}{dy} + \eta_2 \frac{d^2\hat{v}_x}{dy^2} \tag{14}$$

and

$$\hat{T}_1^{xy} = \frac{\eta_1}{1 + \mathrm{We}\,\kappa} \frac{d\hat{v}_x}{dy}\,. \tag{15}$$

Combining the above two equations leads to the following ordinary differential equation:

$$\frac{d^2\hat{v}_x}{dy^2} - \frac{\mathrm{Re}\,\kappa(1 + \mathrm{We}\,\kappa)}{1 + \eta_2\,\mathrm{We}\,\kappa}\,\hat{v}_x = 0\,. \tag{16}$$

The corresponding linearized boundary conditions are:

$$\hat{v}_x = 0\,, \quad \text{at} \quad y = 0 \tag{17}$$

$$\left(\frac{1 + \eta_2\,\mathrm{We}\,\kappa}{1 + \mathrm{We}\,\kappa}\right) \frac{d\hat{v}_x}{dy} = -F'(\bar{v}_w)\,\hat{v}_x\,, \quad \text{at} \quad y = 1. \tag{18}$$

Equations (16)–(18) constitute an eigenvalue problem for the eigenvalue κ which might be complex, because the problem is not self-adjoint. The general solution of Eq. (16) is the sum of terms of the following form:

$$\hat{v}_x(y) = C_1 \sin(my) + C_2 \cos(my)\,, \tag{19}$$

where the constants C_1 and C_2 and the parameter m might be complex. The constant C_2 is zero due to the boundary condition at $y=0$. Imposing the other boundary condition at $y=1$ leads to the characteristic equation

$$\mathrm{Re}\,\kappa \frac{\cot m}{m} = F'(\bar{v}_w) \tag{20}$$

where κ and m are related through the expression

$$m^2 = -\frac{\mathrm{Re}\,\kappa(1 + \mathrm{We}\,\kappa)}{1 + \eta_2\,\mathrm{We}\,\kappa}\,. \tag{21}$$

The system of Eqs. (20) and (21) represents the desired eigenvalue relation. For given values of the parameters (We, Re, η_2), one can calculate the values of κ and m by solving the above system.

The next step is to determine the loci of points such that Real $(\kappa)=0$, i.e. the curves of neutral stability. The critical relationship between the parameters that yields the curve of neutral stability is determined by assuming that κ is imaginary, i.e. $\kappa = i\,\kappa_i$. Equations (20) and (21) then become

$$i\,\mathrm{Re}_\kappa \frac{\cot m}{m} = F'(\bar{v}_w)\,, \tag{22}$$

$$m^2 = -\frac{i\,\mathrm{Re}_\kappa(1 + i\,E\,\mathrm{Re}_k)}{1 + i\,\eta_2\,E\,\mathrm{Re}_k}\,, \tag{23}$$

where

$$\mathrm{Re}_k \equiv \mathrm{Re}\,\kappa_i\,, \tag{24}$$

$$\mathrm{We}_k \equiv \mathrm{We}\,\kappa_i\,, \tag{25}$$

and E is the elasticity number given by

$$E \equiv \frac{\mathrm{We}}{\mathrm{Re}} = \frac{\mathrm{We}_k}{\mathrm{Re}_k}\,. \tag{26}$$

Let now m_r and m_i be the real and imaginary parts of m, respectively. After substituting into Eqs. (20) and (21) and equating real and imaginary parts, one obtains the following system of four equations in six real variables:

$$m_r^2 - m_i^2 = \frac{E\,\mathrm{Re}_k^2(1 - \eta_2)}{1 + \eta_2^2\,E^2\,\mathrm{Re}_k^2}\,, \tag{27}$$

© Steinkopff Verlag 1998

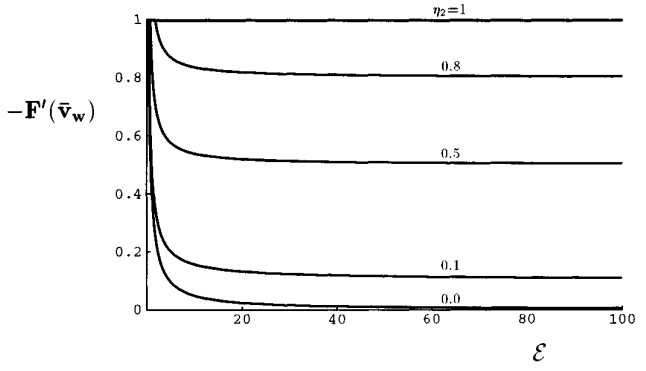

Fig. 2 Stability curves for the shear flow of an Oldroyd-B fluid with slip along the fixed wall. The flow is unstable above the corresponding curve. The curves go to η_2 as $\mathrm{E}\to\infty$

$$2\,\mathrm{m_r}\,\mathrm{m_i} = -\frac{\mathrm{Re_k}\,(1+\eta_2\,\mathrm{E}^2\,\mathrm{Re_k^2})}{(1-\eta_2^2\,\mathrm{E}^2\,\mathrm{Re_k^2})}\,, \tag{28}$$

$$\mathrm{m_i}\,\sinh(2\,\mathrm{m_i}) - \mathrm{m_r}\,\sin(2\,\mathrm{m_r}) = 0\,, \tag{29}$$

$$\mathrm{Re_k}\,\sin(2\,\mathrm{m_r}) + F'(\bar{v}_w)\,\mathrm{m_i}\,(\cos(2\,\mathrm{m_r}) - \cosh(2\,\mathrm{m_i})) = 0\,. \tag{30}$$

To construct the neutral stability curves, we solved the system of Eqs. (27)–(30) using AUTO, a numerical software for continuation and bifurcation in algebraic systems and ordinary differential equations (Doedel et al., 1994). For a given value of η_2, we have chosen the elasticity number E as the continuation parameter. We first solved the system at a high value of E, i.e. E=100, using the Newton-Raphson method and then traced the solution branch for smaller values of E. The neutral stability curves for various values of η_2 are plotted in Fig. 2. Our calculations verified that κ_r changes sign across the curves of Fig. 2, hence these are marginal stability curves (Drazin and Reid, 1985) separating stable from unstable solutions. Steady-state solutions above such a curve are linearly unstable. Furthermore, on the calculated neutral stability curves the imaginary part κ_i of κ is non-zero, which suggests that the time-dependent solution is oscillatory. This is confirmed by the numerical calculations discussed below. It should be emphasized that a small disturbance of a basic solution excites all the modes, whereas the marginal stability curves determine the stability of a single mode. Numerical calculations for the system of Eqs. (27)–(30) and the asymptotic analysis results of the next section verify that this single mode is the most dangerous.

As illustrated in Fig. 2, for a given η_2, the stability of a basic solution is determined from the values of $F'(\bar{v}_w)$ and E. If $F'(\bar{v}_w) > 0$, the solution is stable independently of the value of the elasticity number E. If $F'(\bar{v}_w) < 0$, the solution is unstable if

$$-1 < -F'(\bar{v}_w) < \mathrm{S_{crit}} < 0\,,$$

where $\mathrm{S_{crit}}$ is an increasing function of E. Note that $F'(\bar{v}_w)$ cannot be less than –1 due to our assumption that V_1 is a monotonic function of v_w in steady state. As noted in Georgiou (1996), increasing the value of η_2 reduces the size of the instability regime. Moreover, the Newtonian flow (E=0 or η_2=1) is always stable.

Asymptotic results

In the limit of zero Reynolds number, the shear stress component T_1^{xy} and the velocity gradient $\frac{\mathrm{d}v_x}{\mathrm{d}y}$ are constant and the velocity v_x is linear at all times. It can be then shown that the calculated marginal stability curves approach asymptotically the value η_2 (Georgiou, 1996). In this section, approximate solutions for large values of the elasticity number E are derived. In what follows, the avariables $F'(\bar{v}_w)$, $\mathrm{Re_k}$, and m are assumed to be functions of E and η_2 and will be expanded in a perturbation series lor large E.

Starting with an order of magnitude analysis for m, one observes that the absolute value of m^2 (Eq. (21)) is

$$|\mathrm{m}|^2 = \frac{\mathrm{Re_k}\,\sqrt{1+\mathrm{E}^2\,\mathrm{Re_k^2}}}{\sqrt{1+\eta_2^2\,\mathrm{E}^2\,\mathrm{Re_k^2}}}\,.$$

In the case of large E, the above equation is simplified to

$$|\mathrm{m}|^2 \approx \frac{\mathrm{Re_k^2\,E}}{\eta_2\,\mathrm{Re_k\,E}} = \frac{\mathrm{Re_k}}{\eta_2}\,.$$

If $\mathrm{Re_k} \ll \eta_2$, then $|\mathrm{m}| \ll 1$ and Eq. (21) can be expanded in a Laurent series about $m=0$:

$$\mathrm{i\,Re_k}\,\frac{\cot\mathrm{m}}{\mathrm{m}} = \mathrm{i\,Re_k}\left(\frac{1}{\mathrm{m}^2} - \frac{1}{3} - \frac{\mathrm{m}^2}{45} + \mathrm{O}(\mathrm{m}^4)\right) = F'(\bar{v}_w)\,. \tag{31}$$

It should be pointed out that the case $\eta_2 = 0$ is singular and will be treated separately. The important step here is to reveal the dependency of $\mathrm{Re_k}$ on E. The procedure can be found in any book on singular perturbation techniques (i.e., Holmes, 1991). The correct expansion is of the form

$$\mathrm{Re_k} = \frac{\mathrm{Re_{k_1}}}{\sqrt{\mathrm{E}}} + \frac{\mathrm{Re_{k_3}}}{\mathrm{E}^{3/2}} + \mathrm{O}\left(\frac{1}{\mathrm{E}^{5/2}}\right), \tag{32}$$

where $\mathrm{Re_{k_1}}$ and $\mathrm{Re_{k_3}}$ are functions of η_2 to be determined. Expanding m^2 and $1/m^2$ (Eq. (23)) for large E gives

$$\mathrm{m}^2 = -\mathrm{i}\,\frac{\mathrm{Re_{k_1}}}{\eta_2\,\sqrt{\mathrm{E}}} + \frac{1-\eta_2}{\eta_2^2\,\mathrm{E}} + \mathrm{O}\left(\frac{1}{\mathrm{E}^{3/2}}\right)$$

and

$$\frac{1}{m^2} = i\,\frac{\eta_2\sqrt{E}}{Re_{k_i}} + \frac{1-\eta_2}{Re_{k_1}^2} + i\,\frac{1-\eta_2-\eta_2\,Re_{k_1}\,Re_{k_3}}{\sqrt{E}\,Re_{k_1}^3} + \frac{(\eta_2-1)\,(1+2\,Re_{k_1}\,Re_{k_3})}{E\,Re_{k_1}^4} + O\left(\frac{1}{E^{3/2}}\right).$$

Substituting the above expressions in Eq. (31) and separating into real and imaginary parts lead to the following two expressions:

$$F'(\bar{v}_w) = -\eta_2 + \frac{\eta_2 - 1 - Re_{k_1}^4/(45\,\eta_2)}{E\,Re_{k_1}^2} + O\left(\frac{1}{E^2}\right), \tag{33}$$

and

$$i\,\frac{(3-3\,\eta_2-Re_{k_1}^2)}{3\sqrt{E}\,Re_{k_1}} + O\left(\frac{1}{E^{3/2}}\right) = 0\,. \tag{34}$$

From the latter equation it is easily found that $Re_{k_1} = \sqrt{3-3\,\eta_2}$. Substituting into Eq. (33) gives

$$F'(\bar{v}_w) = -\eta_2 - \frac{(4\,\eta_2+1)}{15\,\eta_2\,E} + O\left(\frac{1}{E^2}\right). \tag{35}$$

This procedure can be pursued to higher orders to obtain:

$$Re_k = \frac{\sqrt{3-3\,\eta_2}}{\sqrt{E}} - \frac{8\,\eta_2^2 - 2\,\eta_2 + 1}{14\,\sqrt{3-3\,\eta_2}\,\eta_2^2\,E^{3/2}} - \frac{2944\,\eta_2^4 - 2976\,\eta_2^3 + 2264\,\eta_2^2 + 324\,\eta_2 - 631}{15\,400\,(3-3\,\eta_2)^{3/2}\,\eta_2^4\,E^{5/2}} + O\left(\frac{1}{E^{7/2}}\right), \tag{36}$$

$$F'(\bar{v}_w) = -\eta_2 - \frac{(4\,\eta_2+1)}{15\,\eta_2\,E} + \frac{48\,\eta_2^2 - 36\,\eta_2 + 23}{1575\,\eta_2^3\,E^2} - \frac{2\,(4991\,\eta_2^3 - 9133\,\eta_2^2 + 4063\,\eta_2 + 2004)}{1\,819\,125\,\eta_2^5\,E^3} + O\left(\frac{1}{E^4}\right). \tag{37}$$

Note that the above expression yields the asymptotic value of $-\eta_2$ as E goes to infinity, in agreement with the analysis of Georgiou (1996).

The case $\eta_2 = 0$ is treated in a similar manner. Equation (23) simplifies to

$$m^2 = Re_k^2\,E - i\,Re_k\,,$$

and thus for large E and small Re_k, one gets $m \approx Re_k\sqrt{E}$. Because, in this asymptotic case, *m* is a real number, the only possible solution of Eq. (22) is $F'(\bar{v}_w) = 0$ with $m = n\pi/2$, $n = 1, 2, \ldots$. Numerical and analytical results revealed that the solution with $m = \pi/2$ corresponds to a broader instability region and hence dictates the stability of a steady-state solution. The corresponding asymptotic result is the following

$$Re_k = \frac{\pi}{2\sqrt{E}} + O\left(\frac{1}{E^{3/2}}\right).$$

As before, we assume an expansion for Re_k of the form (32) and expand $\frac{\cot m}{m}$ about $m = \pi/2$. The procedure for obtaining the higher order approximations is similar to the one used for non-zero η_2 but algebraicaly more complicated. The results are

$$Re_k = \frac{\pi}{2\sqrt{E}} - \frac{3}{4\,\pi\,E^{3/2}} - \frac{(3+4\,\pi^2)}{48\,\pi^3\,E^{5/2}} + O\left(\frac{1}{E^{7/2}}\right),$$

$$F'(\bar{v}_w) = -\frac{1}{2\,E} + \frac{(\pi^2+12)}{24\,\pi^2\,E^2} - \frac{(\pi^4 - 120 + 50\,\pi^2)}{240\,\pi^4\,E^3} + O\left(\frac{1}{E^4}\right). \tag{38}$$

In Fig. 3, we show a comparison between the exact solution of Eqs. (27)–(30) versus the asymptotic solutions (36) and (38). Generally, there is good agreement for all values of E although the present theory was developed for large E.

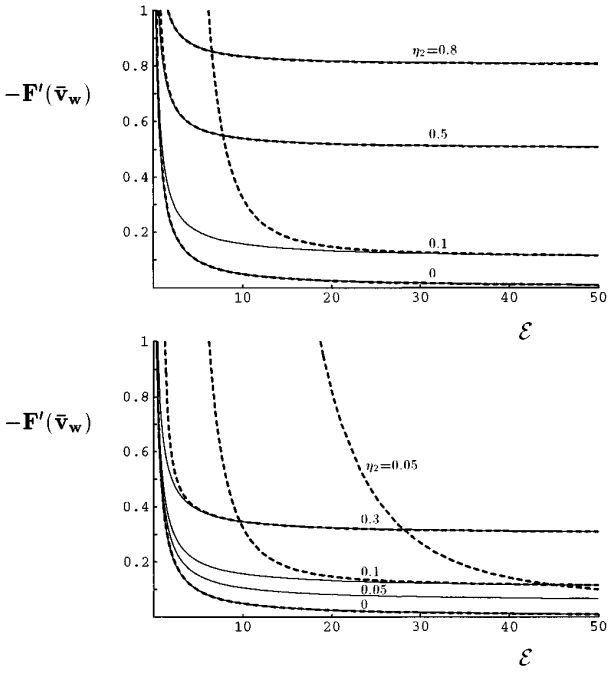

Fig. 3 Comparison between numerical (solid curves) and asymptotic results (dashed curves)

© Steinkopff Verlag 1998

Discussion

The marginal stability curves of Fig. 2 lie below the corresponding curves of Georgiou (1996). The predicted instability regimes are larger and agree quantitatively with the finite element calculations for small sizes of the initial perturbation. The numerical calculations show that perturbing a linearly unstable steady-state solution leads to a periodic solution the amplitude and the period of which increase with elasticity (Georgiou, 1996). A large perturbation may destabilize a linearly stable solution and lead to a periodic solution. In other words, the linearly stable solutions are not necessarily globally stable (Joseph, 1976). Calculating the radius of attraction of conditionally stable steady-state solutions and constructing the global stability curves are out of the scope of the present work. The objective is to demonstrate that the combination of elasticity and nonlinear slip leads to periodic solutions as is the case with the stick-slip instability.

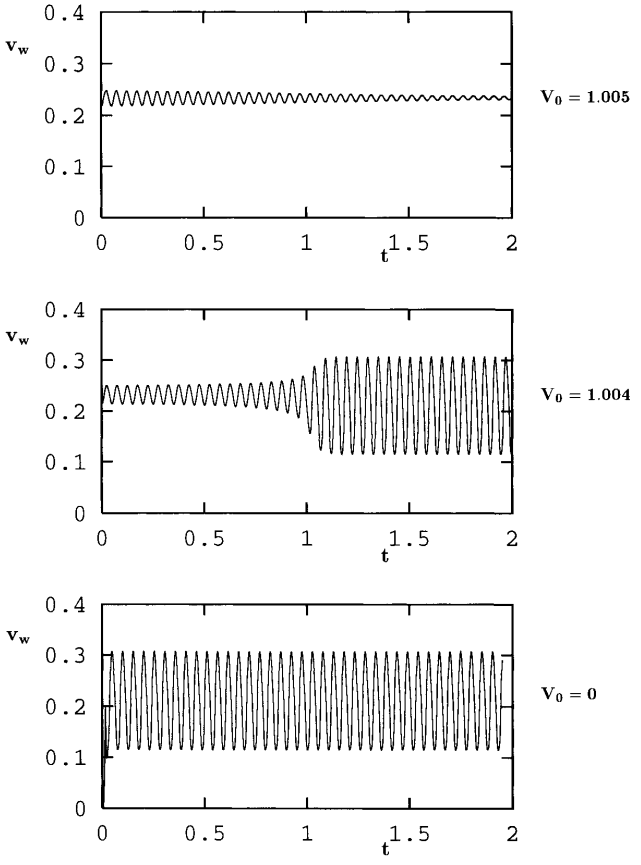

Fig. 4 Evolution of v_w for $V=1.01$, $We=0.0078$, $Re=0.01$, $\eta_2=0.1$ with various initial perturbations: (a) $V_0=1.005$; (b) $V_0=1.004$; (c) $V_0=0$

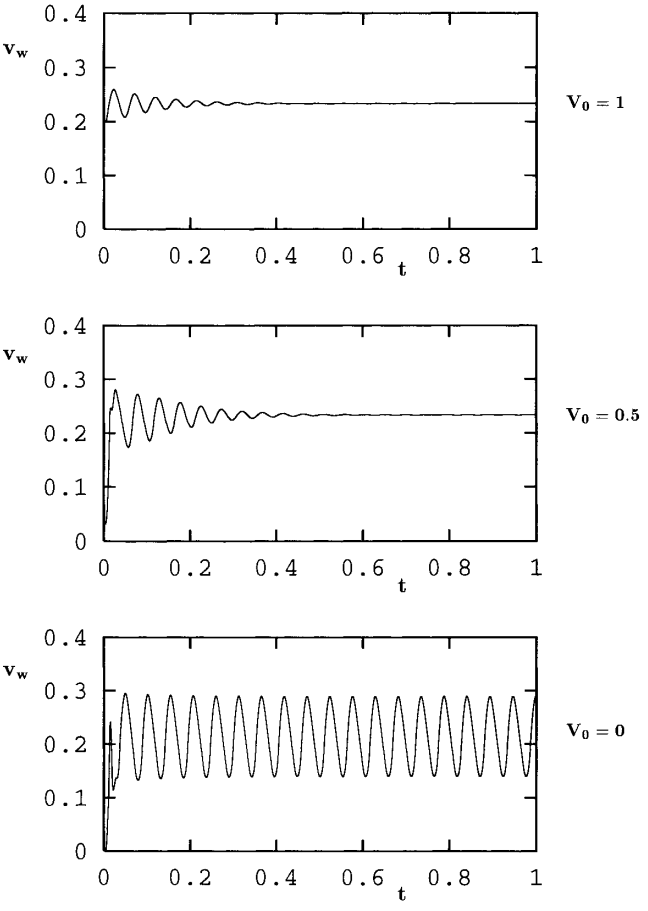

Fig. 5 Evolution of v_w for $V=1.01$, $We=0.007$, $Re=0.01$, $\eta_2=0.1$ with various initial perturbations: (a) $V_0=1$; (b) $V_0=0.5$; (c) $V_0=0$

In order to make comparisons between the linear stability and the numerical results, we employ the following dimensionless slip equation

$$F(v_w) = \mathrm{A}_1 \left(1 + \frac{\mathrm{A}_2}{1 + \mathrm{A}_3\, v_w^2}\right) v_w\,, \tag{39}$$

where $A_1=1$, $A_2=15$ and $A_3=100$ (Georgiou, 1996). With the above choice of parameters, $F(v_w)$ in nonmonotonic as required. Consider the case of $V_1=1.01$, $Re=0.01$ and $\eta_2=0.1$. The linear stability analysis predicts that the flow is marginally stable for $We=0.0078$. From the value of k_i on the marginal curve, one can also obtain the period with which the oscillatory instability sets in, which is equal to $T=2\pi/k_i=0.0496$. In Fig. 4, we plot the evolution of v_w for different initial perturbations, i.e. for $V_0=1.005$, 1.004 and 0, where V_0 is the initial velocity of the lower plate which is changed to V_1 at time $t=0$. In all cases, the time-dependent solution is oscillatory. For small perturbations (i.e., when V_0 is greater than 1.004) the oscillations decay with time and the solution converges to the perturbed

steady-state solution. Note that the calculated period of the decaying oscillations agrees well with the prediction of the linear stability analysis. For smaller values of V_0 (i.e., for larger perturbations), the oscillations grow and the solution becomes periodic at large times (Figs. 4b and c). The amplitude and the period of the periodic solutions is independent of the initial perturbation. An interesting observation is that the period of the periodic solution ($T = 0.0516$) is slightly larger than that of the decaying oscillations obtained for small perturbations.

The effect of the initial perturbation is also illustrated in Fig. 5, where we show results for $V = 1.01$, $Re = 0.01$, $\eta_2 = 0.1$ and $We = 0.007$. The corresponding steady-state solution is linearly stable. The numerical calculations show that for values of V_0 as small as 0.5 the solution converges to the steady-state solution (Figs. 5a and b). However, for larger perturbations (i.e. for $V_0 = 0$, Fig. 5c), the time-dependent solution becomes periodic. For lower values of the Weissenberg number (i.e. for $We = 0.006$), the steady-state solution is stable irrespective of the size of the perturbation, i.e. it is globally stable.

Acknowledgments The authors are grateful to Prof. Marcel Crochet (Université Catholique de Louvain) for his invaluable suggestions and criticism and to Prof. J.R. Anthony Pearson (University of Cambridge) for his comments.

References

Crochet MJ, Davies AR, Walters K (1984) Numerical simulation of non-Newtonian flow. Elsevier Science Publishers

Doedel EA, Wang X, Fairgrieve T (1994) AUTO 94: Software for continuation and bifurcation problems in ordinary differential equations. California Institute of Technology Applied Mathematics Report

Drazin PG, Reid WH (1985) Hydrodynamic stability. Cambridge University Press, Cambridge

Georgiou GC, Crochet MJ (1994a) Compressible viscous flow in slits with slip at the wall. J Rheol 38:639–654

Georgiou GC, Crochet MJ (1994b) Time-dependent compressible extrudate-swell problem with slip at the wall. J Rheol 38:1745–1755

Georgiou GC (1996) On the stability of the shear flow of a viscoelastic fluid with slip along the fixed wall. Rheol Acta 35:39–47

Hatzikiriakos SG, Dealy JM (1992a) Wall slip of molten high density polyethylenes. II. Capillary Rheometer studies. J Rheol 36:703–741

Hatzikiriakos SG, Dealy JM (1992b) Role of slip and fracture in the oscillating flow of HDPE in a capillary. J Rheol 36:845–884

Holmes MH (1991) Introduction to perturbation methods. Springer, New York

Joseph DD (1976) Stability of fluid motions I. Springer, New York

Larson RG (1992) Instabilities in viscoelastic flows. Rheol Acta 31:213–263

Malkus DS, Nohel JA, Plohr BJ (1991) Analysis of new phenomena in shear flow of non-Newtonian fluids. SIAM J Appl Math 51:899–929

Pearson JRA (1985) Mechanics of polymer processing. Elsevier, London